Desalination and Water Treatment
www.deswater.com
doi: 10.5004/dwt.2019.23857

149 (2019) 363–369
May

Application of multispectral remote sensing technology in water quality monitoring

Fei Yin[a,b], Guofan Yang[a,*], Mengdong Yan[c], Qimeng Xie[a]

[a]*College of Water Conservancy, Shenyang Agricultural University, Shenyang, 110866, China, email: 810411678@163.com (G. Yang)*
[b]*College of Water Resources and Civil Engineering, Jilin Agriculture Science and Technology College, Jilin, 132101, China*
[c]*Water Resources Planning and Design Institute, Chaoyang Water Conservancy Bureau, Chaoyang, 122000, China, email: zhangyk2567@126.com*

Received 22 October 2018; Accepted 15 January 2019

ABSTRACT

In order to understand the water quality of the Qinghe Reservoir in a timely and accurate manner, multi-spectral remote sensing technology is used to monitor the water quality. Using the OLI data of Landsat satellite, the correlations of single-band and band combination with the chlorophyll concentration and total suspended solids concentration of OLI data are analyzed by SPSS software. The largest correlation coefficient is selected to construct the ratio linear regression model and the nonlinear least squares support vector machine (LS-SVM). The two models are used to study the multi-spectral remote sensing inversion of chlorophyll a and total suspended solids in Qinghe Reservoir. The results show that compared with the ratio linear regression model, the LS-SVM model increases the decision coefficient R^2 of the predicted and actual chlorophyll a from 0.635 to 0.966, and the root mean square error decreases from 4.83 to 2.67; the coefficient R^2 of the predicted and actual suspended solids concentration is increased from 0.686 to 0.88, and the average relative error is reduced from 3.52% to 3.16%. The accuracy of multispectral remote sensing inversion of the concentration of chlorophyll a and total suspended solids is significantly improved by LS-SVM model.

Keywords: Multi-spectral remote sensing; Water quality; Monitoring; Chlorophyll a; Suspended solids; Least squares support vector machine

1. Introduction

As a large type II reservoir on the main stream of the Qinghe River which is the first-class tributary of the mid-stream of Liaohe River, Qinghe Reservoir undertakes important tasks of flood control, irrigation, fish farming and standby water source. If the water body is in eutrophication state, it will form "green scum" on the surface of the water body, causing fish to die, which seriously affects the water quality of the water body and the operation of the reservoir, so it is particularly important to obtain the water quality of the Qinghe Reservoir accurately, quickly and objectively.

In recent years, the country mainly conducts remote sensing inversion studies on water quality monitoring of large lakes such as Taihu Lake, Qiandao Lake and Wuliangsuhai. For example, the literature proposed to use satellite to monitor the sea chlorophyll a space near the water body and performed time inversion; literature proposed to use the improved quantitative remote sensing technology to monitor inland water quality; literature proposed the use of paper-based sensors and mobile phones for water quality monitoring [1–3]. However, the research methods in these references have less research on the remote sensing water quality of small-area waters such as inland rivers and reservoirs. The relationship between the spectral characteristics of satellite data and the concentration of water quality parameters is analyzed and multi-spectral remote sensing is established. The model is of great significance for the remote

* Corresponding author.

sensing water quality monitoring of inland small-area water bodies [4].

In this paper, the Qinghe Reservoir is used as the research area [5]. The OLI data of Landsat satellite is used to conduct multi-spectral remote sensing inversion of chlorophyll a and suspended solids in Qinghe Reservoir [6–8]. The correlation between band combination and chlorophyll a and suspended matter is analyzed, and the most relevant combination is selected to establish the most suitable multi-spectral remote sensing inversion model to provide a theoretical basis for the remote sensing inversion of chlorophyll a and suspended solids in Qinghe Reservoir [9–12].

2. Materials and methods

2.1. Overview of the study area

Qinghe Reservoir is located in Tieling City, Liaoning Province, with east longitude 124°10′–124°26′, north latitude 42°29′–42°36′. It covers an area of 465.09 km^2 (water area is 47.6 km^2), which is a large reservoir on the Qinghe River, the left-hand tributary of the middle reaches of the Liaohe River. The maximum capacity of the reservoir is 971 million m^3, with the functions of power generation, irrigation, flood control, breeding, tourism and so on. In 2010, the People's Government of Liaoning Province officially listed Qinghe Reservoir as a backup water source. Therefore, it is particularly important to conduct comprehensive and timely monitoring, analysis and evaluation of the water quality of Qinghe Reservoir [13].

2.2. Data acquisition and processing

The data selected in this study include the Landsat satellite OLI data with imaging time of June 23, 2015 and the water sampling data of Qinghe Reservoir acquired on the same day. In order to obtain the sampling data of Qinghe Reservoir, this study randomly selected 25 sampling points in Qinghe Reservoir. The sampling time is from 9:00 to 12:00 on June 23, 2015. The weather is fine. The reservoir is used for actual sampling. The sampling depth is 50 cm below the water surface. The collected water samples are labeled with brown bottles and the longitude and latitude of the sampling points are recorded.

OLI data of Landsat satellite have nine bands. When performing multi-spectral remote sensing inversion of suspended solids concentration in Qinghe, it is especially important to select the appropriate band to construct the model suitable for Qinghe Reservoir. This paper uses the true value of the single-band surface reflectance of pre-processed OLI data and chlorophyll a and suspended solids concentration values at the sampling point of Qinghe Reservoir to make correlation analysis.

The Landsat-8 satellite is a joint launch by the National Aeronautics and Space Administration and the US Geological Survey, which provides reliable data for resources, water, forests, the environment, and urban planning. ENVI software is used for pre-processing of OLI data by radiometric calibration, atmospheric correction, geometric cutting, etc. The main input parameters of atmospheric correction are shown in Table 1:

2.3. Acquisition and pretreatment of sampling point data in Qinghe Reservoir

2.3.1. Acquisition and pretreatment of sampling point data of chlorophyll a in Qinghe Reservoir

2.3.1.1. Extraction method

The collected water sample is filtered by a suction filter [14]. After the suction filtration is completed, the filter membrane is removed and cut into a graduated centrifuge tube, and frozen for 4–8 h. After the freezing, 90% acetone is added to the centrifuge tube and centrifuged. Then the supernatant is added to the cuvette, and the chlorophyll a concentration is obtained by reading with a fluorescent chlorophyll meter.

2.3.1.2. Correlation between water reflectance and chlorophyll a

The analysis found that the bands sensitive to the concentration of suspended solids are blue band (B_2), green band (B_3) and red band (B_4).The near-infrared band (B_5) is sensitive to chlorophyll a difference, but the single-band correlation is not high. By performing the above four bands combination [15]; the band combination with higher correlation is listed and described in Table 2:

2.3.1.3. Establishment of ratio linear regression model of chlorophyll a

In this paper, there are 25 sampling points, and the band combination of 17 sampling points is randomly selected

Table 1
Atmospheric correction input parameters

Input parameter	Parameter value	Input parameter	Parameter value
Latitude/(°)	43.180997	Transit date	June 23, 2015
Accuracy/(°)	123.85833	Transit DMT	27:19.4
Aerosol inversion	2-Band (K-T)	Atmospheric model	Mid latitude summer
Water vapor inversion	Nothing	Visibility/km	40
Minimum memory/MB	100	Ground elevation/km	0.187
Pixel size/m	30	Sensor height/km	705
Aerosol Model	Suburban model	Sensor type	Landsat-8 OLI

Table 2
Correlation analysis of band combination and chlorophyll a concentration

Band combination	S_1	S_2	S_3	S_4	S_5	S_6
Correlation coefficient	0.527	0.595	0.636	0.699	0.705	0.729

Note: $S_1 = B_3 - B_2$; $S_2 = B_3/B_2$; $S_3 = B_4/B_2$; $S_4 = B_5/(B_4 + B_5)$; $S_5 = B_5 - B_4$; $S_6 = B_5/B_4$

for multi-spectral remote sensing inversion of chlorophyll a concentration. The regression analysis is performed by three trends of exponential, linear and polynomial, and the remaining eight are used as verification points. The analysis results are shown in Table 3. It can be seen that the correlation coefficient of the one-dimensional linear model $y = -100.9x + 117.53$ is 0.725, and the value is the highest, indicating that the multi-spectral remote sensing inversion is the best.

2.3.2. Acquisition and pretreatment of sampling data of suspended solids in Qinghe Reservoir

2.3.2.1. Extraction method

The water sample is filtered by a filter with a pore size of 0.45 μm and a vacuum pump. After the filtration is stopped, the filter containing the suspended matter is taken out and placed in a constant weighing bottle and transferred to an oven for drying at 103°C to 105°C for 1 h. It is then transferred to a desiccator, allowed to cool to room temperature, then weighed, repeatedly dried, cooled and weighed until the weight is less than 0.4 mg for twice, and the suspended solids concentration is calculated.

2.3.2.2. Correlation analysis between water reflectance and suspended solids

The analysis found that the bands sensitive to the concentration of suspended solids have blue band (B_2), near-infrared band (B_5) and green band (B_3), and their decision coefficient R^2 are 0.51, 0.505 and 0.399, respectively. The regression analysis of B_2, B_3 and B_5 as independent variables and the single-band regression model did not have accuracy high enough to meet the estimation requirements of the concentration of suspended solids in Qinghe Reservoir.

Table 3
Retrieval model of chlorophyll a concentration in Qinghe Reservoir

Parameter	Inversion model	Correlation coefficient
$x = B_5/B_4$	$y = 419.61x^2 - 847.88x + 449.06$	0.716
	$y = -100.9x^2 - 117.53$	0.725
	$y = -90.11 \ln x + 17.112$	0.719

2.3.2.3. Establishment of ratio linear regression model of suspended solids

Since the linear regression model with single-band as the independent variable has low precision, in order to improve the estimation accuracy of suspended solids concentration, by combining the above three bands, the band combination with higher concentration of suspended solids is selected as the independent variable to establish the suitable model for estimating the concentration of suspended solids in Qinghe reservoir. Through the combination of S_1 = Band(a)/Band(b), the band ratio obtained as a result of B_2/B_5 has the largest correlation in the ratio combination. The model established by using it as an independent variable has a decision coefficient of only 0.331. Through the combination of S_2 = Band(a)/Band(b), the band combination with the result of $B_3 + B_5$ is the most relevant to the suspended solids. The model established by using it as an independent variable has a decision coefficient of only 0.686. Through the combination of S_3 = Band(a) + Band(b) + Band(c), the model with $B_2 + B_3 + B_5$ combination as the independent variable can be obtained a decision coefficient of 0.646. The model established by three forms is shown in Fig. 1. It is generally considered that the decision coefficient can be used to evaluate the quality of the model. The model with $0.5 \le R^2 \le 0.65$ is a poor model; the model with an R^2 between 0.66 and 0.81 is an accurate model. It can be seen from Fig. 1 that the largest decision coefficient is 0.686 in the linear regression model established with B_2, B_3 and B_5 as independent variables, and the standard of the model is the general model.

2.4. Establishment of least squares support vector machine model

Since the linear regression model does not accurately predict the concentration of chlorophyll a and suspended matter in Qinghe Reservoir, in order to more accurately predict the concentration of chlorophyll a and suspended matter in the Qinghe Reservoir, a nonlinear least squares support vector machine model (LS-SVM) is selected, which has great predictive advantages in small sample, nonlinear and high-dimensional pattern recognition [16]. The least squares support vector machine (LS-SVM) is to add an error squared term to the standard support vector machine's objective function. It is a modified version of the standard support vector machine regression process and has a faster solution than the standard SVM, as well as with less computing resources required. The basic principle of it is to map the input vector from the original space to the high-dimensional space through nonlinear mapping and perform linear regression fitting in high-dimensional space [17]. The least squares support vector machine algorithm for function estimation is as follows:

Let the training sample be $D = \{(x_k, y_k) | k = 1, 2, ..., N\}$, $x_k \in R^n$, $y_k \in R$. x_k is the input data and y_k is the output data. The function estimation problem in ω space can be described to solve the following issue:

$$\min_{\omega b e} J(\omega e) = \frac{1}{2}\omega^T\omega + \frac{1}{2}\gamma\sum_{k=1}^{N} e_k^2 \quad (1)$$

where: error variable $e_k \in R$; b is the amount of deviation; γ is the regularization parameter.

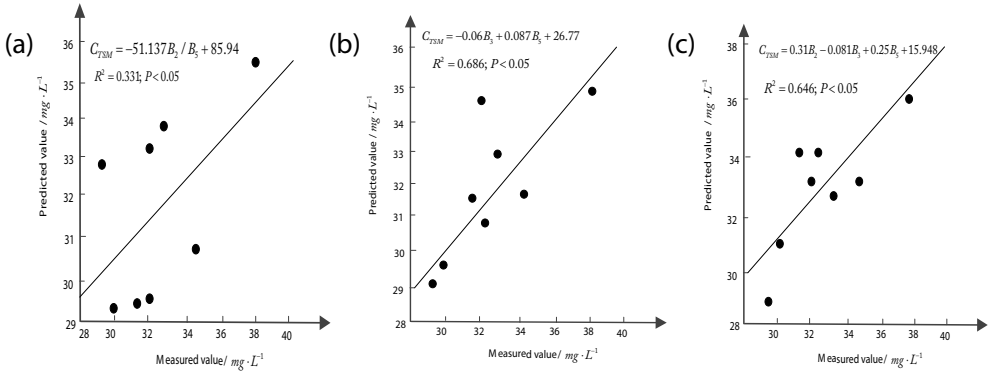

Fig. 1. Regression analysis of total suspended solids concentration and actual value. (a) B_2/B_5 Combination degree model, (b) $B_3 + B_5$ combination degree model and (c) $B_2 + B_3 + B_5$ combination degree model.

The constraint of the above equation is $y_k = \omega^T \varphi(x_k) + b = e_k$, $k = 1, ..., N$, where ω is the weight vector, and φ is the parameter of the kernel space mapping function.

The Lagrangian function is defined as $L(\omega, b, e, a) = J(\omega, e) - \sum_{k=1}^{N} a_k \{\omega^T \varphi(x_k) + b + e_k - y_k\}$, where the Lagrangian multiplier is $a_k \in R$.

The above equation is optimized, and according to the KTT condition, there is:

$$\begin{cases} \dfrac{\partial L}{\partial \omega} = 0 \to \omega = \sum_{k=1}^{N} a_k \varphi(x_k) \\ \dfrac{\partial L}{\partial b} = 0 \to \sum_{k=1}^{N} a_k = 0 \\ \dfrac{\partial L}{\partial e_k} = 0 \to a_k = \gamma e_k \\ \dfrac{\partial L}{\partial a_k} = 0 \to \omega^T \varphi(x_k) + b + e_k - y_k = 0 \end{cases} \tag{2}$$

For $k = 1, ..., N$, eliminating ω and e can get the following equation:

$$\begin{bmatrix} 0 & 1^T \\ 1 & M + \gamma^{-1} I \end{bmatrix} \begin{bmatrix} b \\ a \end{bmatrix} = \begin{bmatrix} 0 \\ Y \end{bmatrix} \tag{3}$$

where: $1 = [1, ..., 1]^T$, $Y = [y_1, ..., y_N]^T$, $a = [a_1, ..., a_N]^T$. M is a square matrix whose elements in the i-th row and j-column are $M_{ij} = \varphi(x_k)^T \varphi(x_j) = M(x_i, x_j)$, and $M(x,y)$ is the kernel function. To find a and b by the least squares method, and the predicted output is:

$$Y(x) = \sum_{k=1}^{N} a_k \varphi(x)^T \varphi(x_k) + b = \sum_{k=1}^{N} a_k M(x, x_k) + b \tag{4}$$

In this paper, all 25 groups of data are processed by MATLAB [18]; and predict is selected as the kernel function of LS-SVM. Among them, 17 groups are used as modeling data, and the remaining 8 groups are used as verification data.

3. Results

3.1. Test results of multi-spectral remote sensing inversion of chlorophyll a in Qinghe Reservoir by using two models

In this paper, 25 sets of experimental data are processed, and 17 sets of data are used to establish two different prediction models of ratio linear regression model and a nonlinear least squares support vector machine model (LS-SVM). The band ratios of the remaining eight sets of data are, respectively, placed in a multi-spectral remote sensing inversion model to calculate the predicted value of chlorophyll a concentration. And the correlation between the predicted value and the actual value is analyzed. The results are described in Fig. 2, and the relative error results are calculated as shown in Table 4:

It can be seen from Fig. 2 that the correlation of the predicted concentration value and the measured value of Chl-a by using the LS-SVM model is $R^2 = 0.966$, and the predicted value of the ratio linear model is $R^2 = 0.6353$. Calculating $\text{RMSE} = \sqrt{\frac{1}{n}\sum_{i=1}^{n}(y_1 - y_0)^2}$ can obtain RMSE = 2.67 for the LS-SVM model and RMSE = 4.83 for the ratio linear regression model.

In this paper, the Landsat-8 satellite and the four bands with high water sensitivity are selected for the inland clean water of Qinghe Reservoir, and the combination $S_6 = B_5/B_4$ with best correlation is used as the independent variable. The multi-spectral remote sensing inversion of the concentration of chlorophyll a in Qinghe Reservoir is carried out by using ratio linear regression model and LS-SVM model, respectively. The results are described in Fig. 2 and Table 4. It can be seen from Fig. 2 and Table 4 that the ratio linear model has the highest correlation. The prediction results of two multi-spectral remote sensing inversion models show that the maximum error of the LS-SVM model is 13.3%, and the error of multi-spectral remote sensing inversion is less than 10%; while the maximum error of the ratio linear model is 29.3%. There are four points of which the spectral remote sensing inversion error is below 10%. And the correlation between the predicted value and the measured value of the LS-SVM model is $R^2 = 0.966$, the root mean square error is RMSE = 2.67, while those of the ratio linear regression model is $R^2 = 0.6353$ and RMSE = 4.83. The correlation between the predicted value and the measured value of the LS-SVM

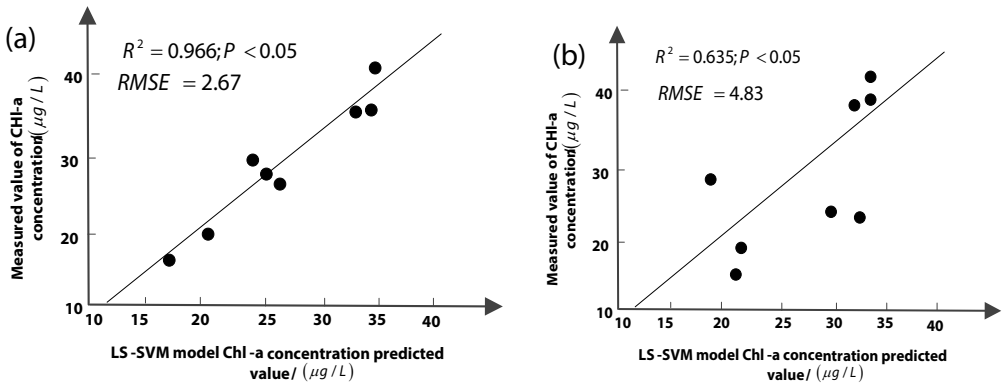

Fig. 2. Correlation analysis between chlorophyll a concentration and actual value. (a) Prediction results of Chl-a concentration in ratio linear model and (b) prediction results of Chl-a concentration in LS-SVM model.

Table 4
Relative error between measured and predicted values of chlorophyll a concentration in samples

CHl-a measured concentration/(μg L^{-1})	Ratio linear regression model		LS-SVM model	
	Forecast/(μg L^{-1})	Relative error/(%)	Forecast/(μg L^{-1})	Relative error/(%)
16.4	21.2	29.3	18.1	10.4
19.6	21.9	11.7	20.4	4.08
28.5	20.3	28.8	24.7	13.3
27.1	30.8	13.7	25.9	4.42
26.5	32.1	21.1	26.6	0.38
36.7	33.8	7.90	33.9	7.63
36.8	35.2	4.35	35.0	4.89
40.4	34.5	14.6	35.3	12.6

model is larger than that of the ratio linear regression model, and the root mean square error is smaller than the ratio linear regression model. Therefore, the prediction effect of the LS-SVM model is better.

Based on this, the LS-SVM model is used to perform multi-spectral remote sensing inversion of the concentration of chlorophyll a in Qinghe Reservoir on June 23, 2015. The concentration distribution is shown in Fig. 3.

It can be clearly seen from Fig. 3 that most of the concentration of chlorophyll a in the Qinghe Reservoir is 15–45 μg L^{-1}, and the concentration of chlorophyll a between 45 and 75 μg L^{-1} is mainly distributed at the edge of the reservoir area. The growth conditions of algae in the edge part of the reservoir area are better than those in the middle part of the reservoir area, and the concentration of chlorophyll a is higher. Because the multi-spectral remote sensing inversion time is June 23, 2015, June is the relatively dry season of Tieling, with less precipitation, which is the most vigorous growth season of algae. Therefore, the concentration of chlorophyll a in the multi-spectral remote sensing inversion of Qinghe Reservoir is relatively high.

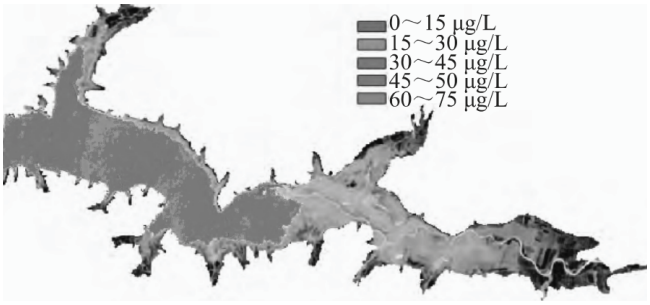

Fig. 3. Distribution of chlorophyll a concentration in Qinghe Reservoir in June 23, 2015.

3.2. Test results of multi-spectral remote sensing inversion of suspended matter in Qinghe Reservoir by two models

In this paper, all single-band and concentration of suspended solids of Landsat-8 is carried out the correlation analysis, and the bands with high correlation obtained areas B_2, B_3, B_5. The single-band model is established to predict the concentration of suspended solids in Qinghe Reservoir. The decision coefficient is $R^2 = 0.51$, $R^2 = 0.399$ and $R^2 = 0.505$, respectively, as shown in Fig. 4:

In Fig. 4, the average relative error of the single-band model for predicting the concentration of suspended solids in Qinghe Reservoir is 5.29%, 6.52% and 4.86%, respectively. Therefore, the model established by using the single-band as an independent variable has a lower decision coefficient and a larger relative error, and which is not suitable for the prediction of concentration of suspended solids in Qinghe Reservoir. In this paper, the ratio linear regression model and the nonlinear LS-SVM model are used to establish the multi-spectral remote sensing inversion of the concentration of suspended

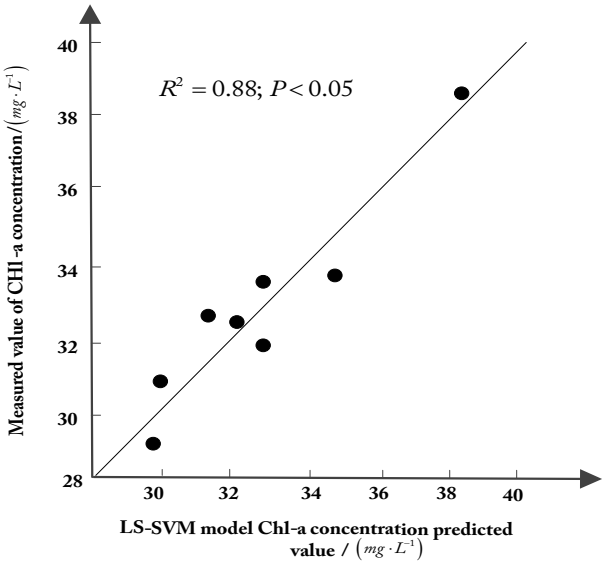

Fig. 4. Regression analysis of predicted and measured values of total suspended solids in LS-SVM model.

solids in Qinghe Reservoir with the band combination of B_2, B_3, B_5 band as the independent variable. In the ratio linear regression model, model $C_{TSM} = 0.06B_3 + 0.087B_5 + 26.77$ with B_3, B_5 as the independent variable has the largest decision coefficient, $R^2 = 0.686$, and the average relative error is 3.25%, because of $C_{TSM} = 0.1B_2 - 0.081B_3 + 0.025B_5 + 15.948$ with B_2, B_3, B_5 as the independent variable and $C_{TSM} = -51.137B_2/B_5 + 85.94$ with B_2/B_5 as the independent variable. Taking B_2, B_3, B_5 as the independent variable and the measured concentration of suspended solid as the dependent variable, the established LS-SVM model can determine the decision coefficient of suspended solids in Qinghe Reservoir by $R^2 = 0.88$, $P < 0.05$, and the average relative error is 3.16%. Therefore, the prediction effect of LS-SVM model is much better than that of the ratio linear regression model.

Based on this, the LS-SVM model is used to perform multi-spectral remote sensing inversion of the concentration of suspended solids in Qinghe Reservoir on June 23, 2015. The concentration distribution is described in Fig. 5:

Under normal conditions, the concentration of suspended solids within 25 mg L^{-1} in water is not harmful to freshwater fish, and fish can be allowed to grow within

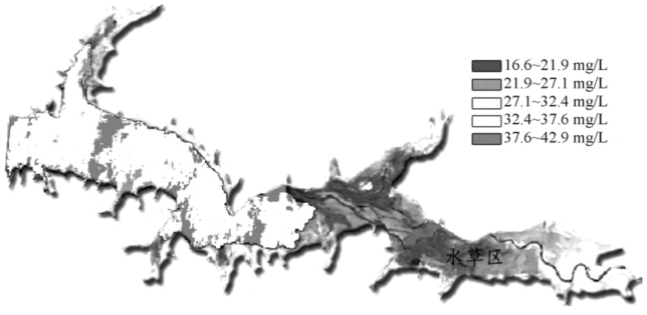

Fig. 5. Distribution of total suspended solids concentration in Qinghe Reservoir in June 23, 2015.

25–80 mg L^{-1}. As shown in Fig. 5, the concentration of suspended solids in Qinghe Reservoir is in the range of 80 mg L^{-1}, and the area with the concentration of suspended solids in 27.1–37.6 mg L^{-1} accounts for most of the Qinghe Reservoir area [19]. The areas where algae and fish activities are relatively strong are mainly distributed in the central part of the reservoir area. Since the multi-spectral remote sensing inversion time is June 23, 2015, June is a relatively dry season in Tieling, precipitation is less, algae growth and fish activities are more vigorous [20]. Therefore, the multi-spectral remote sensing inversion of the concentration of suspended solids in Qinghe Reservoir is relatively higher.

4. Discussion

Multi-spectral remote sensing can not only discriminate the ground object according to the difference of the shape and structure of the image but also discriminate the ground object according to the difference of the spectral characteristics and expand the information amount of remote sensing. Multi-spectral photography for aerial photography and multi-spectral scanning for terrestrial satellites can obtain remote sensing data of different spectral segments [21–24]. The images or data of the spectral segments can be processed by photographic color synthesis or computer image processing, obtaining more abundant images than conventional methods. It also provides the possibility for computer recognition and classification of feature images. In this paper, the results of monitoring the water quality by multi-spectral remote sensing technology show that compared with the linear regression model, the LS-SVM model increases the predicted and actual values of the decision coefficient R^2 of chlorophyll a from 0.635 to 0.966, and the root mean square error decreases from 4.83 to 2.67; the predicted and actual values of the decision coefficient R^2 of suspended solids increased from 0.686 to 0.88, and the average relative error decreased from 3.52% to 3.16%, indicating that the LS-SVM model can improve the multi-spectral remote sensing inversion accuracy of chlorophyll a and total concentration of suspended solids.

5. Conclusion

Because the water quality parameters of remote sensing inversion are affected by many factors, the simple linear model is difficult to adapt to the complex water structure. The prediction result of the nonlinear LS-SVM model is close to the measured chlorophyll a and suspended solids concentration in Qinghe Reservoir. The correlation, the root mean square error, the determinable coefficient and the average relative error of the model are optimized to different degrees compared with those of the linear model. In this paper, multi-spectral remote sensing technology is used to monitor chlorophyll a and suspended solids in Qinghe Reservoir, which provided reference for remote sensing inversion of inland clean water.

References

[1] E.T. Harvey, S. Kratzer, P. Philipson, Satellite-based water quality monitoring for improved spatial and temporal retrieval

of chlorophyll-a in coastal waters, Remote Sens. Environ., 158 (2015) 417–430.
[2] A. Gitelson, F. Szilagyi, K.H. Mittenzwey, Improving quantitative remote sensing for monitoring of inland water quality, Water Res., 27 (2015) 1185–1194.
[3] C. Sicard, C. Glen, B. Aubie, Tools for water quality monitoring and mapping using paper-based sensors and cell phones, Water Res., 70 (2015) 360–369.
[4] R. Altenburger, S. Aitaissa, P. Antczak, Future water quality monitoring—adapting tools to deal with mixtures of pollutants in water resource management, Sci. Total Environ., 512–513 (2015) 540.
[5] M.P. Brahmane, B. Sajjanar, N. Kumar, S.S. Pawar, S.K. Bal, K.K. Krishnani, Impact of rearing temperatures on tilapia oreochromis mossambicus growth, muscle morphology and gene expression, J. Environ. Biol., 38 (2017) 1261–1266.
[6] S.C. Jiang, S.B. Ge, X. Wu, Y.M. Yang, J.T. Chen, W.X. Peng, Treating *n*-butane by activated carbon and metal oxides, Toxicol. Environ. Chem., 99 (2017) 753–759.
[7] L. Kolani, G. Mawussi, D.A. Devault, K. Sanda, Organochlorine pesticide residues in agricultural soils from région des plateaux in togo, Revista Internacional de Contaminacion Ambiental, 33 (2017) 33–42.
[8] L. Liu, X. Cheng, L. Teng, Y. Wang, X. Dong, L. Chen, D. Zhang, W. Peng, Systematic characterization of volatile organic components and pyrolyzates from *Camellia oleifera* seed cake for developing high value-added products, Arabian J. Chem., 11 (2018) 802–814.
[9] C. Mu, P.K. Matsuda, Replication in L2 writing research: journal of second language writing authors' perceptions, TESOL Q., 50 (2016) 201–219.
[10] M. Petrovic, Middle rules and rhumb-line sailing, Polish Marit. Res., 24 (2017) 13–16.
[11] A.S. Cruz, J. Flores, R. Guerra, C. Felipe, E. Lima, Organic biocides hosted in layered double hydroxides: enhancing antimicrobial activity, Open Chem., 16 (2018) 163–169.
[12] D. Tian, L. Sun, L. Zhang, L. Zhang, W. Zhang, L. Li, X. Deng, P. Ning, X. Cheng, J. Deng, G. Hu, Large urban-rural disparity in the severity of two-week illness: updated results based on the first health service survey of Hunan Province, China, Int. J. Equity Health, 15 (2016) 37.
[13] Y. Pica-Granados, G.D. Trujillo, H.S. Hernández, Bioassay standardization for water quality monitoring in Mexico, Environ. Toxicol., 15 (2016) 322–330.
[14] S.J. Halliday, R.A. Skeffington, A.J. Wade, High-frequency water quality monitoring in an urban catchment: hydrochemical dynamics, primary production and implications for the Water Framework Directive, Hydrol. Processes, 29 (2015) 3388–3407.
[15] A.M. Gonçalves, T. Alpuim, Water quality monitoring using cluster analysis and linear models, Environmetrics, 22 (2015) 933–945.
[16] Y. Chang, L. Yan, H. Fang, Anisotropic spectral-spatial total variation model for multispectral remote sensing image destriping, IEEE Trans. Image Process., 24 (2015) 1852–1866.
[17] C.E. Lloyd, J.E. Freer, Using hysteresis analysis of high-resolution water quality monitoring data, including uncertainty, to infer controls on nutrient and sediment transfer in catchments, Sci. Total Environ., 543 (2016) 388–404.
[18] S. Yagur-Kroll, E. Schreuder, C.J. Ingham, A miniature porous aluminum oxide-based flow-cell for online water quality monitoring using bacterial sensor cells, Biosens. Bioelectron., 64 (2015) 625–632.
[19] S. Veeraragavan, R. Duraisamy, S. Mani, Prevalence and seasonality of insect pests in medicinally important plant *Senna alata* L. under tropical climate in the Coromandel Coast of India, Geol. Ecol. Landscapes, 2 (2018) 177–187.
[20] N.J. Raj, A. Prabhakaran, Lineaments of Kodaikanal-Palani massif, Southern Granulitic Terrain of Tamil Nadu, India: a study using SRTM DEM and LANDSAT satellite's OLI sensor's FCC, Geol. Ecol. Landscapes, 2 (2018) 188–202.
[21] W.L. Wun, G.K. Chua, S.Y. Chin, Effect of Palm oil mill effluent (pome) treatment by activated sludge, J. CleanWAS, 1 (2017) 6–9.
[22] O. Adugna, D. Alemu, Evaluation of brush wood with stone check dam on gully rehabilitation, J. CleanWAS, 1 (2017) 10–13.
[23] H. Zarepourfard, A. Aryafar, H. Zia, The investigation of groundwater hydrochemistry of Khezri Plain, South Khorasan Province, Iran. Water Conserv. Manage., 1 (2017) 13–16.
[24] K.A. Halim, E.L. Yong, Integrating two-stage up-flow anaerobic sludge blanket with a single-stage aerobic packed-bed reactorfor raw palm oil mill effluent treatment, Water Conserv. Manage., 2 (2018) 1–4.